*J. Physiol.* (1977), **266**, *pp.* 687–711
*With 9 text-figures*
*Printed in Great Britain*



# THE PASSIVE ELECTRICAL PROPERTIES OF FROG SKELETAL MUSCLE FIBRES AT DIFFERENT SARCOMERE LENGTHS

BY ANGELA F. DULHUNTY* AND CLARA FRANZINI-ARMSTRONG†

*From the Department of Physiology, University of Rochester, Rochester, N.Y. 14642, U.S.A.*

(*Received 18 August 1976*)

SUMMARY

1. The passive electrical properties of frog skeletal muscle fibres have been measured at a number of different sarcomere lengths (from 2·1 to 4·0 $\mu$m). The geometrical outline of each fibre was determined from optical cross-sections and sarcomere length was measured by laser beam diffraction.

2. When fibres were stretched to long sarcomere lengths the membrane capacity, $C_m$, of both normal and detubulated (glycerol-treated) fibres was significantly less than the $C_m$ of fibres at rest length. A significant reduction in membrane conductance of fibres held at long sarcomere lengths was only seen with detubulated fibres.

3. Membrane capacity and membrane conductance have a significant dependence on the cross-sectional area of normal fibres but are independent of cross-sectional area after detubulation.

4. It has been shown that membrane geometry depends on the sarcomere length of the fibre and it is suggested that the passive membrane properties are related to sarcomere length because they depend on membrane geometry.

5. The specific membrane capacity, calculated from the data from detubulated fibres, is 0·8 $\mu$F/cm$^2$.

6. The internal resistivity, $R_i$, of normal fibres, also depends on sarcomere length between 2·1 and 3·0 $\mu$m. At a sarcomere length of 2·1 $\mu$m the average $R_i$ is $122 \pm 3$ $\Omega$.cm (mean $\pm$ S.E. of mean) and at a sarcomere length of 3·0 $\mu$m the average $R_i$ is $210 \pm 17$ $\Omega$.cm (mean $\pm$ S.E. of mean). No further increase in $R_i$ was observed with further increases in sarcomere length.

* Present address: Department of Anatomy, University of Sydney, Sydney, N.S.W. 2006, Australia.

† Present address: Department of Biology, University of Pennsylvania, Philadelphia, U.S.A. 19174.

## INTRODUCTION

The electrical properties of the surface membrane of a skeletal muscle fibre are the lumped properties of the exterior surface membrane and the transverse tubule (T-tubule) membrane. The passive electrical properties of the membrane are usually expressed in terms of the apparent exterior surface area (determined from the geometrical outline of the fibre) and their exact value depends on the true geometry of the membranes. The electrical properties of the surface membrane, expressed in this way, have been shown to vary with changes in surface membrane geometry in two cases. In the first case the passive electrical properties are altered by glycerol-treatment (Gage & Eisenberg, 1969; Eisenberg & Gage, 1969) when the normal continuity between the T-tubules and the fibre exterior is lost (Howell & Jenden, 1967; Howell, 1969; Eisenberg & Eisenberg, 1968). In the second case the electrical properties have been shown to depend on fibre diameter in a way that is consistent with the dependence of T-tubule membrane area on the cross-sectional area of the fibre (Hodgkin & Nakajima, 1972*a*, *b*).

The area of membrane on the exterior surface is significantly greater than the apparent exterior surface area determined from the geometrical outline of the fibre. In addition the ratio of true to apparent exterior surface area decreases with stretch (Franzini-Armstrong & Dulhunty, 1974; Dulhunty & Franzini-Armstrong, 1975*b*; Peachey & Terrell, 1974) and so the passive electrical properties should also change with stretch. Measurements of action potential conduction velocity (Martin, 1954; Hodgkin, 1954) and membrane capacity (Valdiosera, Claussen & Eisenberg, 1974) at different muscle lengths suggest that the electrical properties of the apparent surface of a muscle fibre may vary with sarcomere length. In this paper the passive electrical properties of isolated semitendinosus muscle fibres at different lengths have been systematically determined.

It has been suggested that the internal resistivity, $R_i$, may vary with sarcomere length (M. Schneider, personal communication; Valdiosera *et al.* 1974). The internal myoplasmic resistance, $r_i$, should decrease as the fibre is stretched because of the reduction in cross-sectional area. The specific resistivity should be independent of cross-sectional area if the contents of the fibre were homogeneous. Since the contents are not homogeneous $R_i$ depends on the accessible volume of conducting electrolyte in a unit volume of fibre interior, i.e. the fibre volume minus the volume of myofilaments and sarcoplasmic reticulum. Since the longitudinal current through the fibre is mostly resistive it is probably confined to areas outside the sarcoplasmic reticulum (Schneider, 1970; Mobley, Leung & Eisenberg, 1974, 1975), i.e. the myofibrils. The reduction in the overlap of

thick and thin filaments at long sarcomere lengths might influence the measured $R_1$. In addition the geometry of the sarcoplasmic reticulum must be length dependent and could also influence the measured $R_1$. The results show that there is a significant increase in experimentally determined $R_1$ up to a sarcomere length of 3·0 $\mu$m.

Preliminary reports of some of these results have appeared elsewhere (Dulhunty & Franzini-Armstrong, 1975*a*).

### *Working hypothesis*

The hypothesis is that the passive membrane properties, measured conventionally and normalized to the apparent surface area, depend on sarcomere length in a way that can be predicted from the relation between membrane geometry and sarcomere length. The total surface area of a skeletal muscle fibre consists of the exterior membrane plus the T-tubule membrane and the expected dependence of the geometry of each membrane on sarcomere length is outlined in the next two paragraphs.

*Exterior membrane geometry.* The exterior membrane forms smooth folds and numerous small, permanently open inpocketings called caveolae. The relation between exterior membrane geometry and sarcomere length has been derived in a previous paper (Dulhunty & Franzini-Armstrong 1975*b*). The derivation was based on two assumptions: (*a*) that the fibre has a constant volume and (*b*) that the exterior membrane has a constant total area. The ratio of true exterior membrane area to apparent surface area, $M$, at a fixed sarcomere length is given by $M = 1+\alpha+\beta$ where $\alpha$ is the ratio of the true area of folded membrane to apparent surface area and $\beta$ is the ratio of the true area of caveolar membrane to the apparent surface area. $\alpha$ and $\beta$ vary with sarcomere length, $S$, so that

$$M(S) = 1+\alpha(S)+\beta(S).$$

A graph of $M(S)$, taken from Table 3 of Dulhunty & Franzini-Armstrong (1975*b*) is shown in Fig. 1.

*T-tubule membrane geometry.* Derivation of the relation between T-tubule membrane geometry and sarcomere length depends on the two similar assumptions (*a*) that the fibre has a constant total volume and (*b*) that the T-tubule membrane has a constant total area, $A_T$. The ratio of T-tubule membrane to apparent surface area, $T(S)$, is $A_T/2\pi aNS$ (where $S$ is a standard sarcomere length, $N$ is the number of sarcomeres in the fibre and $a$ is the fibre radius). The ratio of T-tubule membrane to apparent surface area can also be expressed in terms of the T-tubule membrane area per unit fibre volume, i.e. $T = \frac{1}{2}\delta a$ where $\delta$ is the area of T-tubule membrane per unit fibre volume. The ratio of T-tubule membrane to exterior surface membrane, $L(a)$, is a constant function of sarcomere length but depends on fibre size. $L(a)$ is given by $T(S)/M(S)$.

*Membrane capacity.* The capacity of 1 cm² of exterior membrane is called $C_E$ and the capacity of 1 cm² of T-tubule membrane is called $C_w$. Clearly at most sarcomere lengths the capacity of 1 cm² of apparent surface membrane, $C_S$, is given by $C_S = C_E . M(S)$. Similarly, the lumped capacity of T-tubules (per cm² of apparent fibre surface), $C_T$, is given by

$$C_T = C_w T(S) = C_w \tfrac{1}{2}\delta a.$$

The lumped measured membrane capacity, $C_m$, equals $C_S + C_T$, and at the standard sarcomere length, $S$, fibre radius, $a$, and ratio of true to apparent surface area, $M_S$,

$$C_m = M_S C_E + C_w \tfrac{1}{2}\delta a. \quad (1)$$

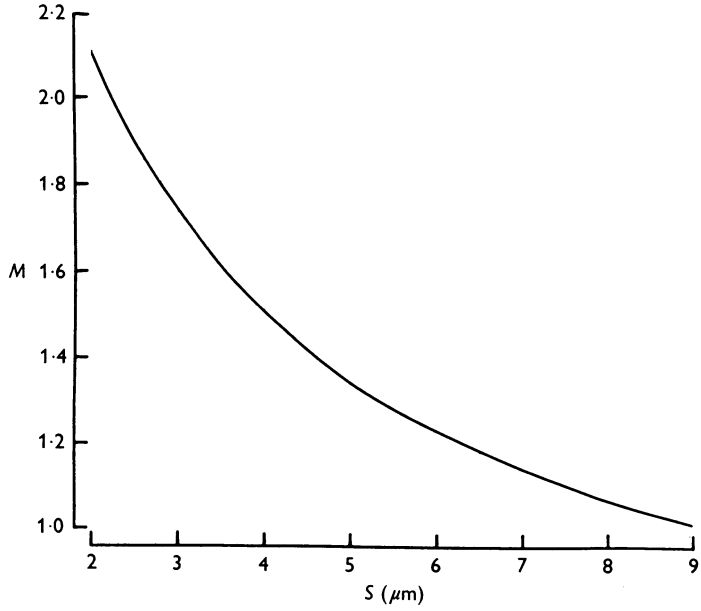


Fig. 1. A graph of the true exterior membrane area per cm² of apparent surface area, $M$ (vertical axis in cm²), against sarcomere length, $S$ (horizontal axis in μm). The constants used to calculate the curve were $M$ equal to 2·12 at a sarcomere length of 2 μm (taken from Table 3 of Dulhunty & Franzini-Armstrong, 1975*b*).

The measurement of $C_m$ may be made at a sarcomere length other than $S$, i.e. $S'$ at which length the fibre radius is $r$ ($r \neq a$). Using constant volume assumptions it can be shown that $C_S$, at $S'$, is equal to $C_E M_S \sqrt{S} \frac{1}{\sqrt{S'}}$, and

$$C_{m'} = C_E M_S \sqrt{S} \frac{1}{\sqrt{S'}} + C_w \tfrac{1}{2}\delta r \quad (2)$$

or

$$C_{m'} = K\frac{1}{\sqrt{S'}} + Hr, \tag{3}$$

where $K$ is a constant for the exterior membrane and $H$ is a constant for the T-tubule membrane.

$C_m$ is only equal to $C_S + C_T$ while the space constant of the T-tubule is equivalent to the fibre radius. If the fibre radius is significantly greater than the T-tubule space constant then eqn. (1) is no longer true. Hodgkin & Nakajima (1972*b*) have shown that eqn. (1) is a reasonable approximation for fibres with diameters less than 100 $\mu$m.

Fibre size was measured experimentally as the ratio of cross-sectional area, $A_{x'}$, to perimeter, $P_{e'}$, and eqn. (3) can be rewritten as

$$C_{m'} = K\frac{1}{\sqrt{S'}} + H\frac{A_{x'}}{P_{e'}} \tag{4}$$

$C_{m'}$ measured experimentally from a number of fibres at one sarcomere length should be a linear function of $A_x/P_e$ and should follow eqn. (4).

In a single fibre $A_x/P_e$ varies with sarcomere length in accordance with the constant volume assumption. Thus for a single fibre eqn. (4) can be rewritten as

$$C_{m'} = K\frac{1}{\sqrt{S'}} + H\sqrt{S}\frac{A_x}{P_e}\frac{1}{\sqrt{S'}}, \tag{5}$$

where $A_x/P_e$ is the fibre size at the standard sarcomere length, $S$. Thus $C_{m'}$ measured from one fibre at various sarcomere lengths, should follow eqn. (5). It was not possible to measure $C_{m'}$; in one fibre at several sarcomere lengths however the size of the fibre at a standard sarcomere length was computed from the measured $A_{x'}/P_{e'}$, using constant volume assumptions, i.e.

$$A_x/P_e = (A_{x'}/P_{e'})(\sqrt{S'}/\sqrt{S}) \tag{6}$$

Fibres having a similar computed size at the standard sarcomere length were compared. In practice this meant that at a sarcomere length of 4 $\mu$m, for example, fibres having an $A_{x'}/P_{e'}$ between 14·1 and 17·4 $\mu$m were plotted on the same graph as fibres having an $A_x/P_e$ between 18 $\mu$m and 20 $\mu$m at a sarcomere length of 2 $\mu$m.

A table of symbols follows, giving definitions of symbols used subsequently in the text.

$S$ sarcomere length ($\mu$m)

$M$ the ratio of the true area of exterior membrane to apparent surface area, $M = 1+\alpha+\beta$

$C_E$ capacity of 1 cm$^2$ of exterior membrane ($\mu$F/cm$^2$)

$C_s$ capacity of 1 cm² of apparent surface membrane, $C_S = M(S)C_E$ ($\mu$F/cm²)

$C_W$ capacity of 1 cm² of T-tubule membrane ($\mu$F/cm²)

$C_T$ capacity of the T-tubules per cm² of apparent surface membrane, $C_T = C_W.T(S)$ ($\mu$F/cm²)

$C_m$ total capacity of the fibre per cm² of apparent surface membrane, $C_m = C_S + C_T = M(S)C_E + T(S)C_w$ ($\mu$F/cm²)

$G_m$ total conductance of the fibre per cm² of apparent surface membrane

$r_i$ resistance of a unit length of fibre interior (Ω/cm)

$R_i$ resistivity of the fibre interior (Ω.cm)

$A_x$ cross-sectional area of fibres, measured from the visible outline of optical cross-sections ($\mu$m)

$P_e$ perimeter of the fibre measured from the visible outline of optical cross-sections ($\mu$m)

## METHODS

Experiments were done on fibres from the semitendinosus muscle of the frog, *Rana pipiens*, and the multiple fibre dissection (Dulhunty & Gage, 1973*a*) allowed isolation of eight to twelve single fibres from each muscle. Fibres had diameters from 40 to 100 $\mu$m and were at least 15 mm long at the shortest sarcomere length. The preparation was mounted on Sylgard (Dow Corning) in a Perspex bath and bathed in a frog Ringer solution which contained (m-mole/l.): NaCl, 115; KCl, 2·5; $CaCl_2$, 1·8; Na phosphate buffer, 3 (pH = 7·2). For the glycerol-treatment experiments, fibres were dissected in normal Ringer and then treated as previously described (e.g. Howell & Jenden, 1967; Gage & Eisenberg, 1969). The preparation remained pinned to the Sylgard throughout the treatment. The solution was changed by removing most of the old solution and then flooding the bath with the new solution. The experiments were done at room temperature 25–36° C.

### *Electrical measurements*

The electrical properties of the fibres were determined by cable analysis (Hodgkin & Rushton, 1946; Fatt & Katz, 1951). Two glass micro-electrodes filled with 3 M-KCl and having resistances from 10 to 20 MΩ were inserted into the fibres, 0·2–1·5 mm apart. A rectangular current pulse was passed through one electrode via a current-clamp circuit (Almers, 1972; C. M. Armstrong, personal communication) and voltage was recorded through the second electrode via a picometric amplifier. The voltage displacement was kept below 6 mV, at the smallest electrode separation, to reduce errors introduced by 'creep' to a minimum. The current and voltage electrodes were placed approximately half way between the tendons. The errors introduced by 'end-effects' at short sarcomere lengths are approximately 2·5 % for the input resistance and space constant and about 5 % for membrane time constant (Hodgkin & Nakajima, 1972*a*). The current and voltage records were obtained on Polaroid film. The input resistance and space constant were obtained graphically from plots of voltage against electrode separation. The time constant was determined from plots of time taken for $V = 0{\cdot}5V_{max}$ against electrode separation (Gage & Eisenberg, 1969). The time constant was also determined from the time taken for $V = 0{\cdot}84V_{max}$

(Hodgkin & Rushton, 1946; Hodgkin & Nakajima, 1972*a*; Adrian & Almers, 1974). Measurements were done on 80 fibres and the time constant determined from the $V = 0{\cdot}84V_{max}$ time was greater than that determined from the $V = 0{\cdot}5V_{max}$ time in fifty-six fibres, was less in sixteen fibres and was the same in eight fibres. On average, the $V = 0{\cdot}84V_{max}$ time constant was 5 % greater than the $V = 0{\cdot}50V_{max}$ time constant. Glycerol-treated fibres were rejected if they had membrane potentials less negative than $-80$ mV or if they showed residual 'creep' (observing hyperpolarizing potentials of 30 mV for 400 msec).

Measurements were taken at one sarcomere length only for each fibre because preparations often deteriorated after a series of micro-electrode penetrations and it was important to keep the preparations in good condition until fixation for subsequent cross-section measurement.

*Measurement of sarcomere length and fibre cross-section*

The sarcomere length of fibres was measured by laser beam ($\lambda = 632$ nm) diffraction (Fig. 2) in the same area of the fibre that had been used for micro-electrode penetration. The sarcomere length was calculated from first order diffraction lines assuming that the sarcomeres act as a simple diffraction grating. Errors were introduced by deflexion of the diffracted beam by the Sylgard and Perspex in the base of the experimental chamber. These were measured experimentally and the final sarcomere length appropriately corrected.

The fibres used for cable analysis were fixed for 1 hr in 0·1 % glutaraldehyde before transfer to an optical chamber (Fig. 2). Fixation produced no change in the fibre's geometry (see Appendix). The fibre cross-section was illuminated using a system similar to that described by Blinks (1965) and Bezanilla & Horowicz (1975). An image of the illuminated cross-section of the fibre was produced by a long working distance 'dry' objective (Leitz, UMK 50, NA 0·6; Fig. 2*B*). The system was calibrated by photographing images of a stage micrometer (Wild) with a 10 $\mu$m spacing. A small error may have been introduced because the micrometer was photographed in air while the fibres were photographed in Ringer solution. The cross-sections of the fibres were enlarged and projected on to tracing paper. Two or three photographs were taken of each fibre at two different magnifications and at least five cross-sections were traced for each fibre. The areas of the cross-sections were measured with a planimeter. Errors are estimated in the Appendix. The error in determination of cross-section is 3·5 % and the error in determination of the perimeter is 1·5 %.

*Linear regression analysis.* The experimental results were initially examined to see whether the measured $C_m$ was in fact related to sarcomere length and fibre size. A linear approximation was made and can be justified for a small range of $S$ and $r$, say from $S$ to $S_1$ and $r$ to $r_1$ using Taylors formula for functions of several variables (see Sokolnokoff & Redheffer, 1958, p. 259).

$$C_m = f(S, r) = f(S_1, r_1) + f_r(S_1, r_1)(r - r_1) + f_S(S_1, r_1)(S - S_1) + R_n, \tag{7}$$

where $R_n$ are terms of higher order which can be ignored if $(S - S_1)$ and $(r - r_1)$ are small. The error introduced by ignoring the remainder increases as $(S - S_1)$ and $(r - r_1)$ become larger. From eqn. 3,

$$f_r(S_1, r_1) = \left(\frac{\partial f}{\partial r}\right)_{S_1, r_1} = H$$

and

$$f_S(S_1, r_1) = \left(\frac{\partial f}{\partial S}\right)_{2S, r_1} = -\frac{K}{2S_1\sqrt{S_1}}.$$

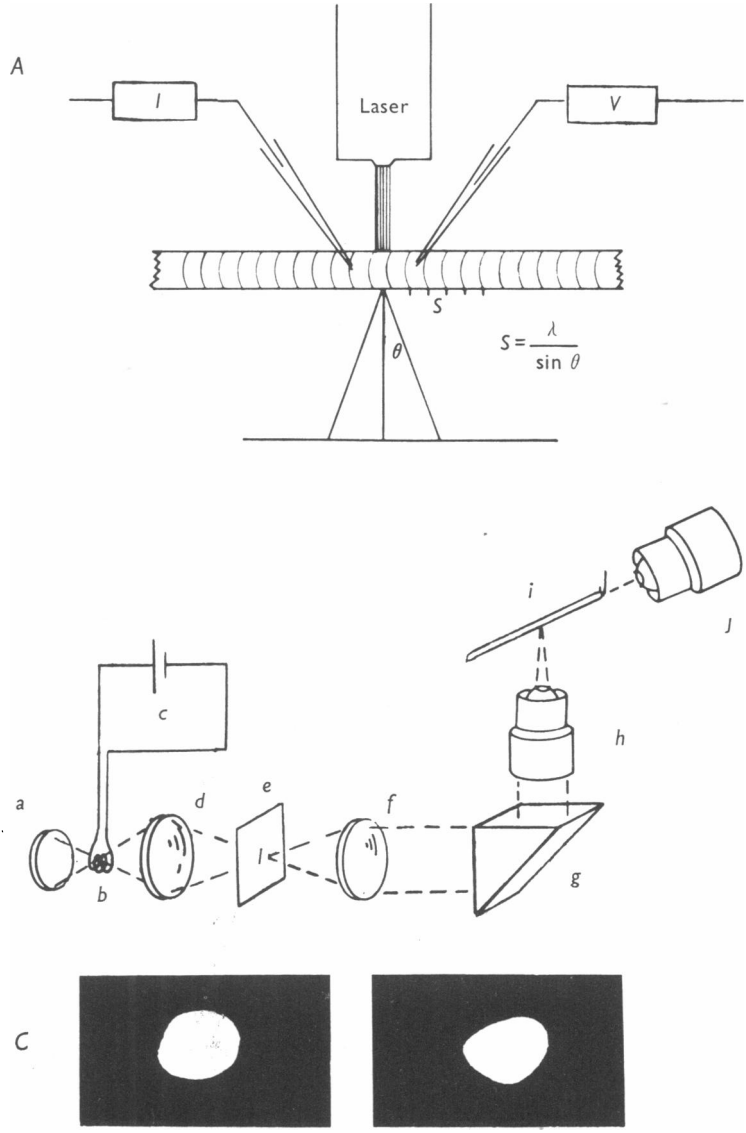


Fig. 2. For legend see opposite.

The first order partial differential of eqn. (3) can therefore be expanded to give

$$C_m = \frac{3K}{2\sqrt{S_1}} + Hr - \frac{K}{2S_1\sqrt{S_1}} . S \tag{8}$$

or

$$C_m = a + br - cS. \tag{9}$$

Experimentally the fibre perimeter, $P_e$, and cross-sectional area, $A_x$, were measured and the equation used is

$$C_m = a + b\frac{A_x}{P_e} - cS. \tag{10}$$

Use of this equation is limited because the error will probably become large when the ranges of $S$ and $r$ are large.

## RESULTS

The membrane capacity, $C_m$ and conductance, $G_m$, per cm$^2$ of apparent fibre surface, were calculated from cable analysis data from eighty normal and twenty-three glycerol treated fibres. The $C_m$ and $G_m$ values were examined with a multiple trend analysis to see if there was a correlation with fibre size or sarcomere length. Eqn. (10) has been used in the analysis so that $C_m$ and $G_m$ are assumed to be linearly related to sarcomere length over the range of lengths used in the experiments (see Methods section).

### (1) *Normal fibres with fibre size*

$C_m$ has been plotted against $A_x/P_e$ in Fig. 3*A* and $G_m$ has been plotted against $A_x/P_e$ in Fig. 3*B*. The results from normal fibres are shown as circles. The trend analysis reveals a close correlation between $C_m$ and fibre size with a significance level less than 0·001 (from $F$ values). There is also correlation between $G_m$ and fibre size with a significance level of 0·002 (from $F$ values). The trend equation for $C_m$ was $C_m = 0{\cdot}094 + 0{\cdot}3A_x/P_e - 0{\cdot}3S$ and the equation for $G_m$ was $G_m = 51{\cdot}32 + 16{\cdot}1A_x/P_e - 2{\cdot}01S$.

---

Fig. 2. Methods used to measure cable properties, sarcomere length and cross-sectional area of single muscle fibres.

*A*, a schematic illustration of sarcomere length measurement in the area of micro-electrode penetration. The He, Ne laser was placed directly above the fibre and the diffraction pattern was observed on the table beneath the bath. Two micro-electrodes are shown, one for passing current from the constant current source, $I$, and the other for recording potential, $V$. The sarcomere length, $S$, was determined from the wave-length of the laser light, $\lambda$, and the angle between the transmitted beam and the diffracted beam, $\theta$, using the equation $S = \lambda/\sin\theta$.

*B*, a schematic illustration of the measurement of fibre cross-section. The fibres were fixed in 0·1 % glutaraldehyde before transfer to this set-up, and suspended in normal Ringer solution while the cross-section was photographed. *a* is a condenser lens with a mirror behind it used to reflect light back into the system. *b* is a quartz-iodine lamp used as a light source and run by the 12 V battery, *c*. *d* is a condenser lens used to focus light on to the slit *e*. *f* is a columnator lens. *g* is a prism. *h* is the first objective lens used to focus light on to the fibre *i*. *j* is the second objective lens attached to the image forming microscope.

*C*, examples of cross-sections photographed with the set-up described in *B*.

The first equation predicts that the surface membrane capacity, $C_s$ (i.e. $C_m$ when $A_x/P_e = 0$), is negative. This is not possible, but may be due to the treatment of $C_m$ as a linear function of $S$ for the purpose of the analysis. Simple regression of data collected at one sarcomere length gives reasonable values for $C_s$ (see Table 1).

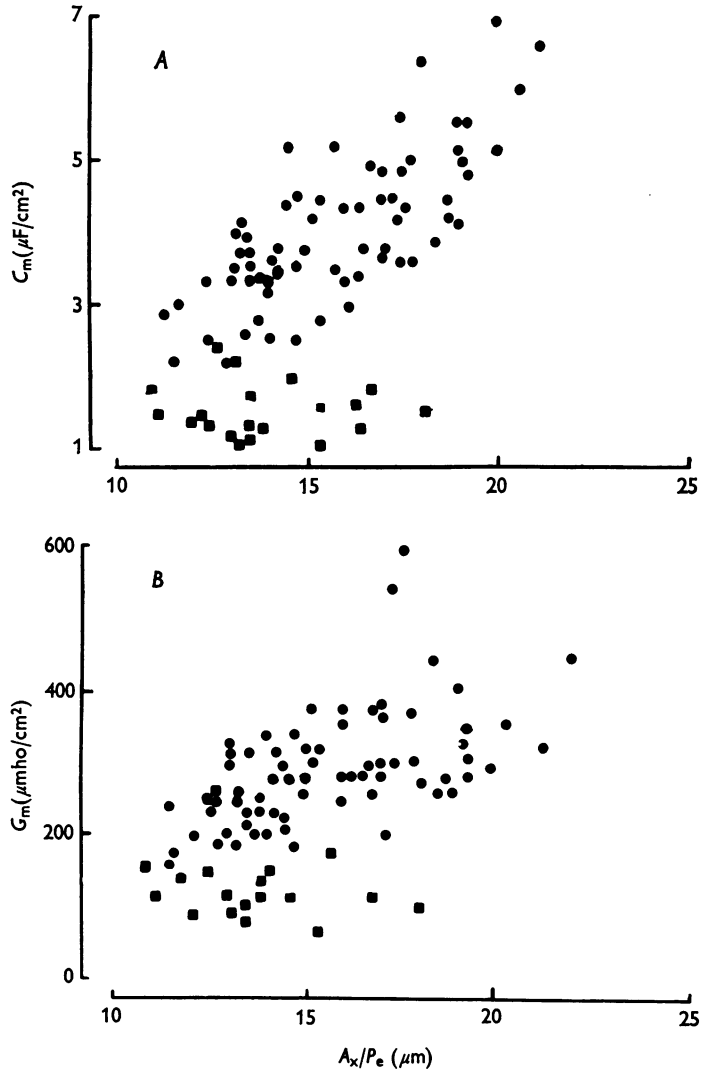


Fig. 3. Experimentally determined passive membrane properties plotted against fibre size, $A_x/P_e$. Graph $A$: membrane capacity, $C_m$ (μF/cm²). Graph $B$: membrane conductance data, $G_m$ (μmho/cm²). Circles: results from normal fibres. Squares: results from glycerol-treated fibres.

(2) *Glycerol-treated fibres and fibre size*

The results obtained from glycerol-treated fibres have been plotted against $A_x/P_e$ in Fig. 3*A* and *B* (squares). Trend analysis of glycerol treated data showed that both $C_m$ and $G_m$ are independent of fibre size. The trend equation for $C_m$ is $C_m = 3{\cdot}4 - 0{\cdot}06\,A_x/P_e - 0{\cdot}47S$ and for $G_m$ is $G_m = 278 - 4A_x/P_e - 32S$.

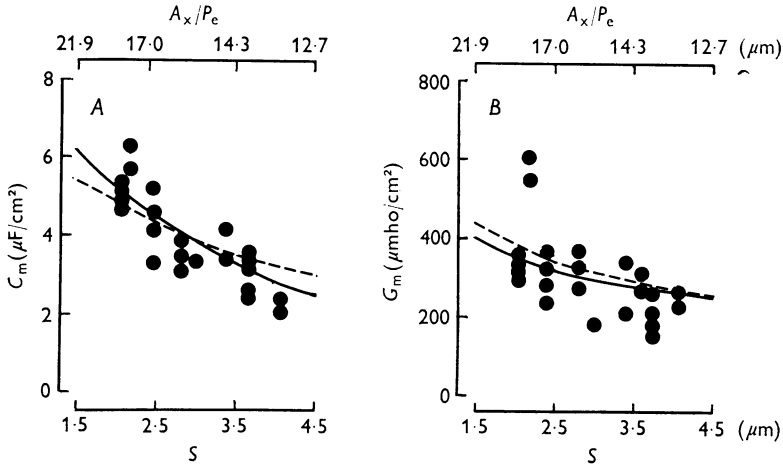


Fig. 4. Experimentally determined passive membrane properties for normal fibres plotted against sarcomere length, *S*. Graph *A*: membrane capacity, $C_m$ (μF/cm²). Graph *B*: membrane conductance, $G_m$ (μmho/cm²). In both graphs the upper horizontal axes show the centre range values of $A_x/P_e$ from which fibres were selected at each sarcomere length (see working hypothesis). In *A*, the continuous curve was calculated from the trend equation for $C_m$ (see text), using values of $A_x/P_e$ and *S* as shown on the horizontal axes of the graph. The broken curve was calculated from eq. (5). Sarcomere length is the only variable in eqn. (5) and so $C_{m2}$ at sarcomere length $S_2$ is simply related to $C_{m1}$ at sarcomere length $S_1$ by the equation $C_{m2} = C_{m1}\sqrt{(S_1/S_2)}$. $C_m$ of 5·4 μF/cm² at a sarcomere length of 1·5 μm was used as a constant for the calculation. In *B*, the continuous curve was calculated from the trend equation for $G_m$ (see text) again using corresponding values for $A_x/P_e$ and *S*. The interrupted curve was calculated in a similar way to that in *A* using assumptions outlined in the working hypothesis. $G_m$ of 440 μmho/cm² at a sarcomere length of 1·5 μm was used as a constant for the calculation.

(3) *Normal fibres and sarcomere length*

The trend analysis on all normal fibres showed that membrane capacity depends on sarcomere length with a significance level of 0·048. Normal membrane conductance does not have a statistically significant dependence on sarcomere length. $C_m$ is plotted against *S* in Fig. 4*A* and $G_m$ is plotted

against $S$ in Fig. 4*B*. Only fibres with a calculated $A_x/P_e$ between 18 and 20 $\mu$m (equivalent diameters of 72–80 $\mu$m) at a sarcomere length of 2·0 $\mu$m were used in the graph for reasons given in the working hypothesis. The average $C_m$ of the fibres shown in Fig. 4*A* is $5{\cdot}01 \pm 0{\cdot}38$ $\mu$F/cm$^2$ (mean $\pm$ S.E. of mean) at a sarcomere length of 2·1 $\mu$m, while at a longer sarcomere length of 3·7 $\mu$m the average $C_m$ is $3{\cdot}12 \pm 0{\cdot}2$ $\mu$F/cm$^2$ (mean $\pm$ S.E. of mean). The restriction on the size of fibres used in Fig. 4 means that the data are taken from a smaller sample of fibres than that used in the trend analysis. There is still a significant reduction in $C_m$ between sarcomere lengths of 2·1 $\mu$m and 3·7 $\mu$m ($t$ test; $P < 0{\cdot}03$).

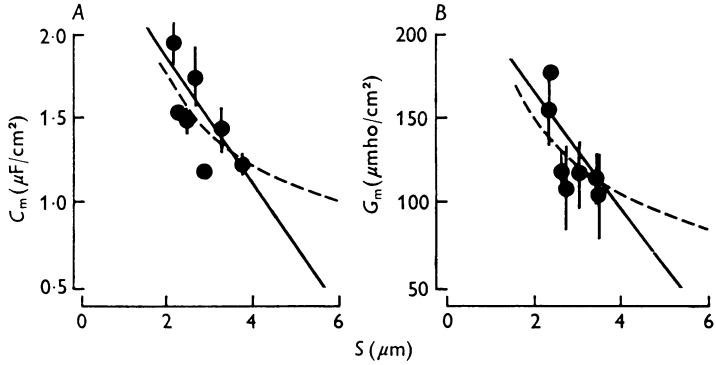


Fig. 5. Passive membrane properties of glycerol-treated fibres plotted against sarcomere length, $S$. Graph $A$: membrane capacity, $C_m$ ($\mu$F/cm$^2$). Graph $B$: membrane conductance, $G_m$ ($\mu$mho/cm$^2$). Each dot shows the average $C_m$ or $G_m$ of fibres at that sarcomere length and the vertical bars indicate $\pm$ S.E. of mean. The continuous curve in $A$ was calculated from the trend equation for $C_m$ from glycerol-treated fibres (see text), assuming an average $A_x/P_e$ of 13 $\mu$m. The broken curve in $A$ was calculated from eqn. (5) modified for fibres without transverse tubules, i.e. $C_{m'} = (1/\sqrt{S'})\,K$. Since $K$ is a constant $C_{m2}$ at a sarcomere length $S_2$ is related to $C_{m1}$ at a sarcomere length $S_1$ by the equation $C_{m2} = C_{m1}\sqrt{(S_1/S_2)}$. $C_m$ of 1·75 $\mu$F/cm$^2$ at a sarcomere length of 2·0 $\mu$m was used as a constant for the calculation. The continuous curve in $B$ was calculated from the trend equation for $G_m$ from glycerol-treated fibres (see text), assuming an average $A_x/P_e$ of 13 $\mu$m. The interrupted curve in $B$ was calculated in a similar way to the broken curve in $A$. A $G_m$ of 150 $\mu$mho/cm$^2$ at a sarcomere length of 2·0 $\mu$m was used as a constant for the calculation.

The average $G_m$ of fibres in Fig. 4*B* is $293 \pm 14$ $\mu$mho/cm$^2$ (mean + S.E. of mean) at a sarcomere length of 2·1 $\mu$m and $236 \pm 21$ $\mu$mho/cm$^2$ (mean $\pm$ S.E. of mean) at a sarcomere length of 3·8 $\mu$m. The continuous lines of both graphs in Fig. 4 have been calculated from the trend equations and the interrupted lines have been calculated from equations derived in the working hypothesis.

(4) *Glycerol-treated fibres and sarcomere length*

The results from glycerol-treated fibres are shown in Fig. 5*A* and *B*. Trend analysis reveals that $C_m$ depends on sarcomere length with a significance level of 0·03 and that $G_m$ depends on sarcomere length with a significance level of 0·06. In Fig. 5*A* the average $C_m$ values for glycerol-treated fibres at each sarcomere length have been plotted. The vertical bars indicate ± S.E. of mean. A reduction in $C_m$ with increasing length is obvious. At a sarcomere length of 2·3 $\mu$m, $C_m$ is 1·85 ± 0·12 $\mu$F/cm$^2$ (mean ± S.E. of mean: three fibres) and at a longer sarcomere length of 3·8 $\mu$m, $C_m$ is 1·2 ± 0·04 $\mu$F/cm$^2$ (mean ± S.E. of mean; two fibres).

Fig. 5*B* shows the average $G_m$ for glycerol-treated fibres at different sarcomere lengths. The vertical bars show ± S.E. of mean. Despite the large standard errors there is a decrease as the sarcomere length increases. At a sarcomere length of 3·8 $\mu$m, $G_m$ is 154 ± 18 $\mu$mho/cm$^2$ (mean ± S.E. of mean; three fibres) and at a sarcomere length of 3·8 $\mu$m, $G_m$ is 105 ± 24 $\mu$ho/cm$^2$ (mean ± S.E. of mean; two fibres). The continuous lines on both graphs in Fig. 5 have been calculated from the trend equations and the interrupted lines have been calculated from equations derived in the working hypothesis. No further statistical analysis has been done; however the calculated quadratic curve appears to give a better fit to the data than the linear approximation. This is in contrast to Fig. 4 where the normal data appear to be fitted equally well by either curve and shows again that the $C_m$ data from glycerol-treated fibres better support the assumptions made in the working hypothesis.

*The electrical properties of the exterior membrane*

$C_m$ from glycerol-treated fibres is a close approximation to the capacity of the exterior membrane, per cm$^2$ of apparent fibre surface $C_s$, if all the T-tubule membrane has been isolated from the surface. Incomplete detubulation after glycerol-treatment has been reported (Eisenberg & Eisenberg, 1968; Gage & Eisenberg, 1969; Nakajima, Nakajima & Peachey, 1973; Valdiosera *et al.* 1974; Franzini-Armstrong *et al.* 1973), however, the fraction of T-tubules remaining connected to the surface is generally small. It is reasonable to suppose that the dependence of $C_m$ on sarcomere length, after glycerol-treatment, is largely due to a dependence of $C_s$ on sarcomere length (see eqn. (3) in the working hypothesis). An independent estimate of $C_s$ can be obtained from normal fibres if $C_m$ has a significant dependence on fibre size (Hodgkin & Nakajima, 1972*a*). Linear regression analysis has been done on data from normal fibres at different sarcomere lengths and the results are given in Table 1. The intercept, slope and correlation coefficient are listed for each sarcomere length.

TABLE 1. Capacity of the exterior membrane

| Normal fibres | | | | | | Glycerol-treated fibres | | | |
|---|---|---|---|---|---|---|---|---|---|
| Sarcomere length ($\mu$m) | Intercept of regression line $\mu$F/cm$^2$ ($\pm$S.E. of mean) $C_s$ | Slope of regression line $\mu$F/cm$^3$ ($+$S.E. of mean) | Correlation coefficient $r^2$ | $M$ | $C_E$ $\mu$F/cm$^2$ | Sarcomere length ($\mu$m) | $M$ | $C_m$ $\mu$F/cm$^2$ (S.E. of mean) | $C_E$ $\mu$F/cm$^2$ |
| 2·07 | 1·4 ($\pm$0·25) | 0·2 ($\pm$0·09) | 0·9 | 2·09 | 0·67 | — | — | — | — |
| 2·12 | 1·6 ($\pm$0·53) | 0·25 ($\pm$0·16) | 0·8 | 2·06 | 0·78 | 2·3 | 1·98 | 1·85 ($\pm$0·15) | 0·93 |
| 2·40 | 1·5 ($\pm$0·20) | 0·11 ($\pm$0·20) | 0·6 | 1·94 | 0·77 | 2·4 | 1·94 | 1·51 | 0·78 |
| 2·80 | 1·5 ($\pm$0·16) | 0·13 ($\pm$0·07) | 0·8 | 1·80 | 0·83 | 2·65 | 1·84 | 1·70 ($\pm$0·22) | 0·92 |
| 3·00 | 1·3 ($\pm$0·17) | 0·17 ($\pm$0·15) | 0·8 | 1·74 | 0·74 | 2·75 | 1·80 | 1·48 ($\pm$0·05) | 0·82 |
| 3·40 | 1·3 ($\pm$0·37) | 0·19 ($\pm$0·13) | 0·6 | 1·63 | 0·80 | 3·1 | 1·70 | 1·18 ($\pm$0·02) | 0·69 |
| 3·70 | 1·1 ($\pm$0·30) | 0·23 ($\pm$0·14) | 0·8 | 1·57 | 0·70 | 3·4 | 1·63 | 1·32 ($\pm$0·12) | 0·81 |
| 3·80 | 0·9 ($\pm$0·31) | 0·10 ($\pm$0·07) | 0·7 | 1·55 | 0·58 | 3·8 | 1·55 | 1·01 ($\pm$0·05) | 0·65 |
| 4·10 | 0·7 ($\pm$0·12) | 0·13 ($\pm$0·06) | 0·8 | 1·49 | 0·58 | — | — | — | — |
| | | | | Average | 0·71 | | | Average | 0·80 |

The intercepts ($C_s$) decrease as sarcomere length increases; however the standard errors are large and there is not a significant difference between $C_s$ at short sarcomere lengths and $C_s$ at long sarcomere lengths. Thus only the results from glycerol-treated fibres support the hypothesis that exterior membrane unfolding will reduce $C_s$ at long sarcomere lengths.

The specific capacity of the exterior membrane, $C_E$, has been calculated from $C_m$ in glycerol-treated fibres and $C_s$ in normal fibres. The ratio of exterior membrane to apparent fibre surface, $M$, was determined in a previous paper (Dulhunty & Franzini-Armstrong, 1975*b*) and is illustrated in Fig. 1. $C_m$ of glycerol-treated fibres (and $C_s$ of normal fibres) is expressed in terms of 1 cm$^2$ of apparent fibre surface; thus, values for $C_E$ can be calculated by dividing the $C_m$ at a particular sarcomere length by $M$ for that sarcomere length. The calculation assumes that all elements of the exterior membrane are electrically continuous. $C_E$ has been calculated for normal and glycerol-treated fibres (see Table 1). Less weight must be given to the $C_E$ calculated for normal fibres because the calculation assumes that the exterior membrane capacity depends on sarcomere length and a significant dependence on sarcomere length has only been shown with glycerol-treated fibres. $C_E$ can also be calculated assuming that $C_s$ is independent of sarcomere length. The average of $C_s$ values given in Table 1 is 1·26 $\mu$F/cm$^2$ and this divided by $M$ for sarcomere length of 2·4 $\mu$m gives $C_E$ of 0·63 $\mu$F/cm$^2$. In either case $C_E$ for normal fibres is lower than $C_E$ for glycerol-treated fibres and this is consistent with a T-tubule remnant remaining connected to the fibre surface after glycerol-treatment. If the true exterior and T-tubule capacity is taken to be 0·71 $\mu$F/cm$^2$ the area of T-tubule remnant can be calculated from equations given in the *Working hypothesis* section. If the fibre radius at a sarcomere length of 2·5 $\mu$m is assumed to be 50 $\mu$m then the difference between $C_E$ for normal and glycerol-treated fibres, 0·09 $\mu$F/cm$^2$, must be due to 3·5% of the normal T-tubule membrane area.

*Internal resistivity as a function of sarcomere length*

The internal resistance, $r_i$, was determined for fibres at each sarcomere length and the specific resistivity, $R_i$, was calculated using the cross-sectional area measured directly from optical sections. The average $R_i$ at each sarcomere length is shown in Fig. 6 (filled circles). The vertical bars represent ± S.E. of mean. $R_i$ increases steeply between sarcomere lengths of 2 and 3 $\mu$m, and maintains a constant value with further stretch up to a sarcomere length of 4 $\mu$m. At a sarcomere length of 2·1 $\mu$m $R_i$ is 122 ± 3·0 ohm.cm (mean ± S.E. of mean) and at a sarcomere length of 2·8 $\mu$m $R_i$ is equal to 207 ± 14 ohm.cm (mean ± S.E. of mean). The difference between these two values of $R_i$ is statistically significant ($t$ test; $0{\cdot}02 < P$

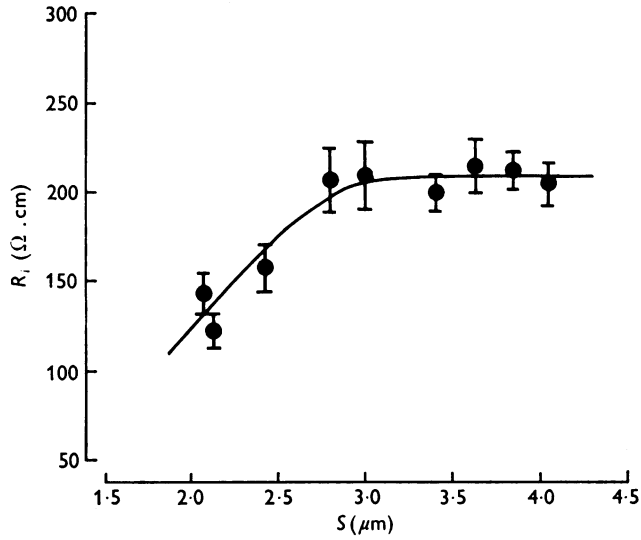


Fig. 6. A graph of the internal resistivity, $R_i$, (Ω/cm) against sarcomere length, $S$. Average results for all normal fibres are shown (filled circles) and the vertical bars represent ± 1 S.E. of mean. The curve has been drawn through the points by eye.

> 0·05). The average values of $R_i$ remained between 190 and 210 Ω.cm for all longer sarcomere lengths up to 4·1 μm.

## DISCUSSION

The results show that the lumped surface membrane capacity, related to the apparent fibre surface area, is a function of sarcomere length as well as fibre cross-section. It is suggested that the dependence on sarcomere length follows changes in the geometry of the exterior and T-tubule membranes. The capacity of the exterior membrane measured in glycerol-treated fibres is also a function of sarcomere length and presumably follows changes in exterior membrane geometry. Structural analysis of the exterior membrane (Dulhunty & Franzini-Armstrong, 1975*b*) has shown that the geometrical changes in normal fibres are a flattening of folds at sarcomere lengths less than 3·2 μm and opening and flattening of caveolae at longer lengths. The caveolae are open at short lengths after glycerol treatment and so changes in the geometry of the exterior membrane are probably simply flattening of folded caveolar and non-caveolar membrane. Hodgkin & Nakajima (1972*a*, *b*) have shown that membrane capacity is related to fibre size because of the dependence of T-tubule geometry on fibre size.

One assumption made in the *Working hypothesis* is that all areas of the

exterior membrane are electrically continuous. Continuity is obvious in glycerol-treated fibres where the caveolae are opened into 'dome' structures. Normally the caveolar 'neck' could provide an 'access' resistance to the lumen. The fact that glycerol-treated fibres have a higher $C_m$ than the $C_s$ from normal fibres (see Table 1) could result from isolation of the caveolar membrane in normal fibres. However, previous investigations (Eisenberg & Eisenberg, 1968; Franzini-Armstrong *et al.* 1973; Nakajima *et al.* 1973) suggest that detubulation is never 100% complete. A T-tubule remnant provides an adequate and simple explanation for the measured value of $C_m$ after glycerol-treatment.

The membrane capacity reported for simple cells, e.g. the squid axon is about 1 $\mu$F/cm$^2$ (Cole, 1940), and biological membranes are thought to generally have a higher capacity than artificial lipid bilayers. The capacity of artificial membranes is about 0·6 $\mu$F/cm$^2$ (Fettiplace, Andrews & Hayden, 1971; Coster & Simons, 1970). If it is assumed that the lipid in biological membranes is in a bilayer (Singer, 1971) then one possible explanation for the higher specific capacity of the biological membrane is that the width of the lipid bilayer is less than that of the artificial membrane (Fettiplace *et al.* 1971). The results presented in this paper indicate that the capacity of the exterior membrane of skeletal muscle is about 0·7 $\mu$F/cm$^2$ and is not sufficiently different from the capacity of the lipid bilayer to suspect a difference in thickness. It is also possible that the surface membrane of the squid axon is not perfectly smooth and that the reported value of 1 $\mu$F/cm$^2$ is an overestimate of the true capacity. A specific exterior membrane capacity of 0·7 $\mu$F/cm$^2$ can be related to the dielectric constant of the plasmalemma. If the plasmalemma thickness is 5 nm, then the dielectric constant is 4·6, which is reasonable.

There is a lot of variation in reported values for internal resistivity and it is becoming apparent that this parameter is sensitive to a number of variables including temperature (Hodgkin & Nakajima, 1972*a*), season (Dulhunty & Gage, 1973*a*) and sarcomere length (this paper). Recently reported values for $R_i$ are listed in Table 2 and the sarcomere length and the temperature at which the measurement was made are also listed. The list is short because it is confined to normal amphibian sartorius and semitendinosus fibres. Muscle length reported in each paper has been converted to sarcomere length.

Normally experiments are done on fibres that have been stretched to a specified percentage of either their slack length or their rest length. We found that the slack sarcomere length for frog sartorius fibres is 1·8 $\mu$m and the rest sarcomere length, measured *in situ*, is 2·4 $\mu$m. For frog semitendinosus fibres the slack length is 2·1 $\mu$m and the rest length is 2·6 $\mu$m. The sarcomere lengths at which measurements were made, $S$, can be calculated by multiplying either the slack length or the rest length by the percentage stretch. All results can thus be standardized to a sarcomere length

of, for example, 2·4 $\mu$m by multiplying the reported value of $S_s$ or $G_s$ by $\sqrt{(S/2{\cdot}4)}$ (using the assumption that the fibre has a constant volume).

All results have been converted to $R_i$ at 26° C using a $Q_{10}$ of 1·37 (Hodgkin & Nakajima, 1972*a*). In the last column of Table 2 values for $R_i$ have been taken from Fig. 6.

TABLE 2. Internal resistivity reported for normal fibres in normal Ringer solution

| Author | Muscle | $S$ ($\mu$m) | $T$ (° C) | $R_i$ ($\Omega$.cm) | *$R_i$ ($\Omega$.cm) | Our $R_i$ ($\Omega$.cm) |
|---|---|---|---|---|---|---|
| Hodgkin & Nakajima (1972*a*) | Sartorius | 2·07 | 18 | 177 | 139 | 130 |
| | Semitendinosus | 2·30 | 18 | 203 | 156 | 150 |
| Dulhunty & Gage (1973*a*) | Sartorius (W) | 2·34 | 20 | 194 | 159 | 155 |
| Bastian & Nakajima (1974) | Sartorius | 2·08 | 20 | 148 | 121 | 130 |
| Schneider† (1970) | Sartorius (S) | 2·65 | 20 | 130 | 106 | 170 |
| Dalhunty & Gage (1973*a*) | Sartorius (S) | 2·34 | 20 | 147 | 121 | 150 |

(S) measurements made in Summer.

(W) measurements made in Winter

* to convert $R_i$ to *$R_i$ (at 26° C) a Q10 of 1·37, as determined by Hodgkin & Nakajima (1972*a*), was used.

† Schneider (1970) reported $R_i$ = 102 $\Omega$.cm in 7·5 mM-$K^+$ at 24° C. Hodgkin & Nakajima (1972) mention that this is equivalent to 130 $\Omega$.cm in normal Ringer at 20° C.

There is good agreement between our data and data reported in the first three papers for both sartorius and semitendinosus fibres (Hodgkin & Nakajima, 1972*a*; Dulhunty & Gage, 1973*a*; Bastian & Nakajima, 1974). When the same measurements are made in summer the results are significantly different (Schneider, 1970; Dulhunty & Gage 1973*a*).

Part of the error in calculation of $R_i$ comes from the use of a geometrical outline and some authors have preferred to use a standard $R_i$. The results presented in Table 2 show that use of a standard $R_i$ may bring in larger errors than those arising from geometrical assumptions unless the conditions of measurement of the standard $R_i$ are identically reproduced. For example, the value reported by Schneider (1970) for summer $R_i$ is 60 % less than the corresponding $R_i$ in this paper and is 30 % less than the average $R_i$ reported by Hodgkin & Nakajima (1972*a*). By comparison, the measurement of one dimension of the fibre and assumption of a circular cross-section can result in errors of about 25 % in cross-sectional area and hence $R_i$ (Blinks, 1965; Dulhunty & Gage, 1973*a*). The measurement of

two dimensions and assumption of an elliptical cross-section reduces the error to between 4 and 10 % (Gordon, Huxley & Julian, 1966; Hodgkin & Nakajima, 1972*a*; Appendix to this paper).

That most longitudinal current must flow through areas occupied by myofibrils has been discussed in the Introduction. It is tempting to try to fit the observed changes in $R_1$ to some length dependent characteristic of the myofilaments. Two such characteristics are the area of fibre cross-section occupied by the myofilaments and the area of overlap between thick and thin filaments. X-ray diffraction data have shown that the volume of the sarcomere is independent of sarcomere length (Huxley, 1953) and therefore as the centre to centre spacing decreases the fraction of a sarcomere occupied by a thick or a thin filament in the area of overlap increases. However, the volume of conducting material remains approximately constant because the decrease in volume as the filaments are forced together is almost exactly matched by an increase in conducting volume as the area of myofilament overlap is reduced. If current is actually conducted along the myofilaments then conduction from thick to thin filaments could depend on the area of overlap. There is overlap of myofilaments to sarcomere lengths of 3·6 $\mu$m. The increase in $R_1$ reaches a maximum at a sarcomere length of about 3 $\mu$m and this is not consistent with the idea of $R_1$ depending on myofilament overlap. The final possibility is that the measured $R_1$ is influenced by the geometry of the sarcoplasmic reticulum. It is difficult to assess this possibility since there is little information available on the behaviour of the sarcoplasmic reticulum during stretch.

## APPENDIX

### *The geometrical outline of muscle fibres*

The Appendix provides a detailed description of the optical procedures used to measure fibre outline for analyses described in the main paper. The optical set-up is illustrated in Fig. 2 of the Methods section.

(1) *Preparation for optical measurements*

Experimental fibres were fixed so that there was no chance of their being damaged during measurement of optical cross-section. The effect of fixation on the cross-sectional area was determined by following the fixation of single living fibres mounted in the optical chamber. Photographs were taken in normal Ringer solution and during fixation in Ringer solution containing 0·1 %, 0·2 % or 0·5 % glutaraldehyde and records were obtained up to 12 hr after the solution change. The concentrations of glutaraldehyde are much lower than those normally used for

electron-microscopy (2·6 %), but they are sufficient to turn the fibres into rigid structures. The fibres did not contract during fixation.

The average area of three to five optical sections photographed before fixation, are expressed as a percentage of the control value in Table 3. 0·1 and 0·2 % glutaraldehyde do not cause measurable changes in the cross-sectional area, but 0·5 % glutaraldehyde causes a small but significant shrinkage, from 4 to 8 % of the control. Examples are illustrated in Fig. 7. The fibres did not change shape Fibres used for electrical measurements were fixed in 0·1 % glutaraldehyde

TABLE 3. Effect of fixation on fibre cross-section

| Glutaraldehyde concn. (%) | No. of fibres | No. of cross-sections | $A_x$ of fixed fibre (% control) mean +S.E. of mean |
|---|---|---|---|
| 0·1 | 2 | 12 | 102 ± 6 |
| 0·2 | 1 | 5 | 99 ± 5 |
| 0·5 | 4 | 17 | 92 ± 5 |

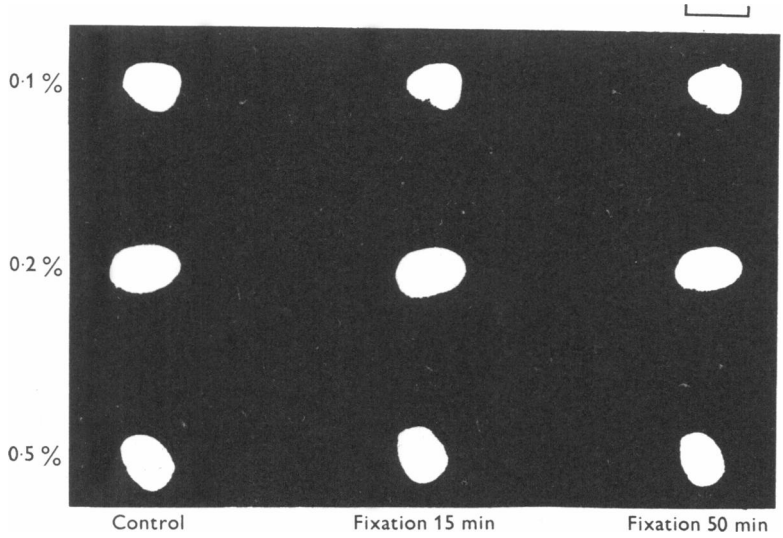


Fig. 7. The effect of fixation in different concentrations of glutaraldehyde on fibre cross-section. Three concentrations of glutaraldehyde were used, 0·1, 0·2 and 0·5 % (made up in normal Ringer solution). The unfixed fibres were first photographed in normal Ringer (first column) and then 15 min (second column) and 50 min (third column) after fixation. The calibration bar is 100 $\mu$m.

(2) *Estimates of errors in optical outlines*

There are four sources of error in obtaining accurate images of fibre outline

(*a*) The orientation of the slit image, the fibre and the image forming microscope were critical. The slit image had to be set at 90° to the long axis of the fibre and the fibre had to be oriented at 90° to the image forming surface in order to focus the whole cross-section on one plane. Fibres with uneven illumination were rejected.

(*b*) The sharpness of the edges depends on precise focusing of the slit image on the fibre as well as focusing the illuminated cross-section by the image forming microscope.

(*c*) Connective tissue could often not be distinguished from the sarcolemma. Areas with a clean outline could be located under the dissecting microscope, and those areas illuminated with the slit image. Fixed fibres could be cleaned more carefully and measurements on these preparations were more accurate.

(*d*) Tracing the photographed sections and subsequent measurements with the planimeter and map measuring devices were subject to error which could only be reduced by repeating measurements and taking average values.

The last two errors (*c* and *d*) were estimated as the percentage variation of cross-sectional areas of each fibre. For thirty-five optical sections from seven fibres, the standard error of the mean cross-section was 1·45 % and the standard error of the mean perimeter was 0·57 %.

(3) *Variation in cross-sectional area along a single fibre*

Cross-sections were normally photographed at one point only. Variations in cross-section were estimated in two fibres by tracking along their length and photographing cross-sections every 1 mm. Two or three photographs were taken at each position. The results from one fibre are illustrated in Fig. 8. The fibres changed shape along their length and appeared to rotate around their long axis. The cross-sectional area, perimeter and ratio of cross-sectional area to perimeter do not show gross variations. The average cross-sectional areas have standard errors of $\pm 2{\cdot}6$ % and $\pm 1{\cdot}1$ % (for fibres 1 and 2 respectively), the average perimeters have standard errors of $\pm 1{\cdot}6$ and $\pm 0{\cdot}72$ % (fibres 1 and 2 respectively), and the average ratio of cross-sectional area to perimeter has standard errors of 1·8 and 0·68 % (fibres 1 and 2 respectively).

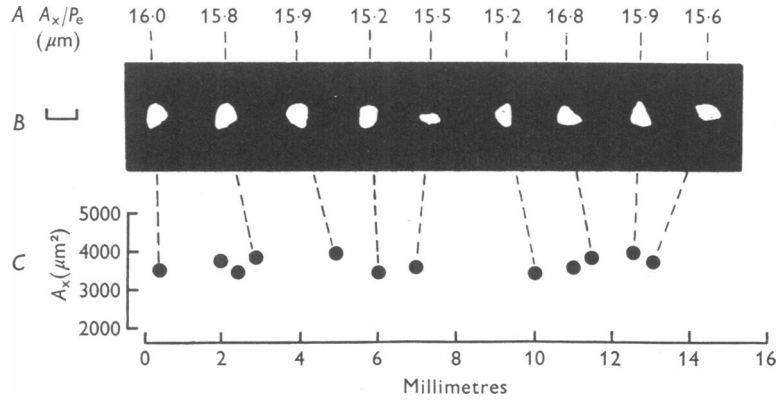


Fig. 8. Variation in cross-section along the length of a fibre. The cross-sections shown in *B* were taken at various intervals along the fibre which had a total length of 14 mm. *C* is a graph of cross-sectional area, $A_x$ (in $\mu m^2$) against distance along the fibre from one tendon (in mm). Some of the cross-sections are shown in *B* and the areas to which they correspond are indicated by the dashed lines going to *C*. The ratio $A_x/P_e$ (in $\mu m$) is shown above each cross-section in *A*.

The calibration bar in *B* is equal to 100 $\mu$m.

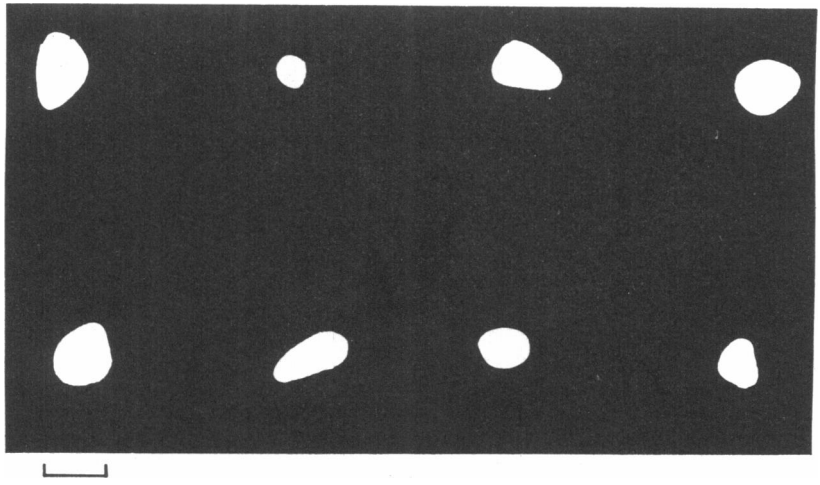

Fig. 9. Examples of the variety of shapes and sizes of stretched fibres. The fibres were fixed at a sarcomere length of 3·4 to 3·8 $\mu$m and were photographed within 4 hr of fixation. Calibration bar is 100 $\mu$m.

(4) *Variations in shape and cross-section with stretch*

The fact that skeletal muscle fibres vary in both size and shape (Blinks, 1965) presents problems in defining the specific electrical properties of muscle fibres (Blinks, 1965; Schneider, 1970; Hodgkin & Nakajima, 1972*a*; Dulhunty & Gage, 1973*b*). The variation in size and shape of fibres from muscles fixed at sarcomere lengths of 3·4–3·8 $\mu$m is illustrated in Fig. 9. The percentage deviation of the fibres from a circular cross-section is given in Table 4. In addition, it was of interest to see whether fibres become more circular when they are stretched.

The fibres used in these calculations were all fixed and optical sections could only be obtained at one sarcomere length.

The fibres are divided into five groups of increasing sarcomere lengths (Table 4, column 1), and containing approximately the same number of fibres (21–27). An equivalent radius, $r'$, was calculated from the measured cross-sectional area, $A_x$, i.e. $r' = \sqrt{(A_x/\pi)}$. An equivalent perimeter, $P'_e$ was calculated from the equivalent radius, again assuming that the fibre has a circular cross-section, i.e. $P'_e = 2\pi r'$. The true perimeter, measured from optical sections, $P_e$, was then compared with the perimeter calculated from assumptions of circular cross-section, $P'_e$. The ratio $P_e/P'_e$ is 1 when the cross-section is circular. Departure from a circular cross-section will increase the ratio, i.e. $P_e/P'_e > 1$. On average, the ratio of $P_e/P'_e = 1{\cdot}06$ so that the calculated perimeter is 6 % smaller than the measured perimeter and thus the error involved in assuming a circular cross-section is 6 % for the perimeter.

TABLE 4. Ratio of measured over calculated perimeters at different sarcomere lengths

| Sarcomere length range ($\mu$m) | No. of fibres | *$P_e/P'_e$ Mean ± S.D. |
|---|---|---|
| 2·1–2·25 | 22 | 106 ± 3 |
| 2·5–2·9 | 27 | 106 ± 3 |
| 3·1–3·45 | 25 | 106 ± 3 |
| 3·5–3·8 | 21 | 105 ± 3 |
| 3·85–4·25 | 18 | 104 ± 4 |

* $P_e$ is the true measured perimeter of the fibre. $P'_e$ is the perimeter calculated from assumption of a circular outline.

The fibres do not become more circular as they are stretched from 2·1 to 4·1 $\mu$m. There is an apparent decrease in $P_e/P'_e$ at the longest sarcomere length, but this is not statistically significant. The decrease seems to be due to a group of fibres from one muscle fixed at 4·1 $\mu$m, that have unusually circular cross-sections.

In conclusion fibres do not increase their suface area by becoming more round as length increases to 4·1 $\mu$m and estimates of cross-sectional area and perimeter, from assumptions of circular cross-section, are not more accurate at long sarcomere lengths.

We thank Dr Paul Horowicz and Dr Francisco Bezanilla for allowing us to use their optical equipment. We are grateful to Dr M. Schneider, Dr C. Armstrong, Dr P. Horowicz, Dr P. Gage and Dr D. Van Helden for their discussion and interest in the experiments. We are indebted to Dr P. Barry for his help with data analysis and to Dr P. Gage, Dr R. H. Adrian and Dr D. Davey for their comments on the manuscript.

The work was supported by a grant from the Muscular Dystrophy Associations of America and by a NIH, IPO, INS 1098 01 grant.

## REFERENCES

ADRIAN, R. H. & ALMERS, W. (1974). Membrane capacity measurements on frog skeletal muscle in media of low ion content. *J. Physiol.* **237**, 573–605.

ALMERS, W. (1972). Potassium conductance changes in skeletal muscle and the potassium concentration in the transverse tubules. *J. Physiol.* **225**, 33–56.

BASTIAN, J. & NAKAJIMA, S. (1974). Action potential in the transverse tubules and its role in the activation of skeletal muscle. *J. gen. Physiol.* **63**, 257–278.

BEZANILLA, F. & HOROWICZ, P. (1975). Fluorescence intensity changes associated with contractile activation in frog skeletal muscle stained with Nile Blue A. *J. Physiol.* **246**, 709–735.

BLINKS, J. R. (1965). Influence of osmotic strength on cross-section and volume of isolated single muscle fibres. *J. Physiol.* **177**, 42–57.

COLE, K. S. (1940). Permeability and impermeability of cell membranes for ions. *Cold Spring Harb. Symp. quant. Biol.* **8**, 110–122.

COSTER, H. & SIMONS, R. (1970). Anomolous dielectric dispersion in bimolecular lipid membranes. *Biochim. biophys. Acta* **203**, 17–27.

DULHUNTY, A. F. & FRANZINI-ARMSTRONG, C. (1975*a*). Variations in internal resistivity with sarcomere length in frog semi-tendinosus fibres. *Biophys. J.* **15**, 130.

DULHUNTY, A. F. & FRANZINI-ARMSTRONG, C. (1975*b*). The relative contributions of folds and caveolae to the surface membrane of frog skeletal muscle fibres at different sarcomere lengths. *J. Physiol.* **250**, 513–541.

DULHUNTY, A. F. & GAGE, P. W. (1973*a*). Electrical properties of toad sartorius fibres in summer and winter. *J. Physiol.* **230**, 619–641.

DULHUNTY, A. F. & GAGE, P. W. (1973*b*). Differential effects of glycerol treatment on membrane capacity and excitation–contraction coupling in toad sartorius fibres. *J. Physiol.* **230**, 619–641.

EISENBERG, B. & EISENBERG, R. S. (1968). Selective disruption of the sarcotubular system in frog sartorius muscle. *J. cell Biol.* **39**, 451–467.

EISENBERG, R. S. & GAGE, P. W. (1969). Ionic conductances of the surface and transverse tubule membranes of frog sartorius fibers. *J. gen. Physiol.* **53**, 279–297.

FATT, P. & KATZ, B. (1951). An analysis of the end-plate potential recored with an intracellular electrode. *J. Physiol.* **115**, 320–370.

FETTIPLACE, R., ANDREWS, D. M. & HAYDEN, D. A. (1971). The thickness composition and structure of some lipid bilayers and artificial membranes. *J. Membrane Biol.* **5**, 277–297.

FRANZINI-ARMSTRONG, C. & DULHUNTY, A. F. (1974). Contribution of folds and caveolae to the surface area of frog muscle fibres: a freeze fracture study. *J. cell Biol.* **63**, 104.

FRANZINI-ARMSTRONG, C., VENOSA, R. A. & HOROWICZ, P. (1973). Morphology and accessibility of the transverse tubular system in frog sartorius muscle after glycerol-treatment. *J. Membrane Biol.* **5**, 277–296.

GAGE, P. W. & EISENBERG, R. S. (1969). Capacitance of the surface and transverse tubule membrane of frog sartorius muscle fibers. *J. gen. Physiol.* **53**, 265–277.

GORDON, A. M., HUXLEY, A. F. & JULIAN, F. J. (1966). Tension development in highly stretched muscle fibres. *J. Physiol.* **184**, 143–169.

HODGKIN, A. L. (1954). A note on conduction velocity. *J. Physiol.* **125**, 221–224.

HODGKIN, A. L. & NAKAJIMA, S. (1972*a*). The effect of diameter on the electrical constants of frog skeletal muscle fibres. *J. Physiol.* **221**, 105–120.

HODGKIN, A. L. & NAKAJIMA, S. (1972*b*). Analysis of the membrane capacity in frog muscle fibres. *J. Physiol.* **221**, 121–136.

HODGKIN, A. L. & RUSHTON, W. A. H. (1946). The electrical constants of a crustacean nerve fibre. *Proc. R. Soc.* B **133**, 444–479.

HOWELL, J. N. (1969). A lesion of the transverse tubules of skeletal muscle. *J. Physiol.* **201**, 515–533.

HOWELL, J. N. & JENDEN, J. D. (1967). T-tubules of skeletal muscle: morphological alterations which interrupt excitation-contraction coupling. *Fedn Proc.* **26**, 553.

HUXLEY, H. E. (1953). X-ray analysis and the problem of muscle. *Proc. R. Soc.* B **141**, 59–62.

MARTIN, A. R. (1954). The effect of change in length on conduction velocity. *J. Physiol.* **125**, 215–220.

MOBLEY, B. A., LEUNG, J. & EISENBERG, R. S. (1974). Longitudinal impedance of skinned frog muscle fibres. *J. gen. Physiol.* **63**, 625–637.

MOBLEY, B. A., LEUNG, J. & EISENBERG, R. S. (1975). Longitudinal impedance of single frog muscle fibres. *J. gen. Physiol.* **65**, 97–113.

NAKAJIMA, S., NAKAJIMA, Y. & PEACHEY, L. D. (1973). Speed of repolarization and morphology of glycerol-treated frog muscle fibres. *J. Physiol.* **234**, 465–481.

PEACHEY, L. D. & TERRELL, A. (1974). Surface area of frog muscle fibres at different sarcomere lengths. In *Proc. Int. Union of Physiol. Sci.*, vol. XI. New Delhi.

SCHNEIDER, M. (1970). Linear electrical properties of the transverse tubules and surface membrane of skeletal muscle fibers. *J. gen. Physiol.* **56**, 640–671.

SINGER, S. J. (1971). The molecular organization of biological membranes. In *Structure and Function of Biological Membranes*, ed. ROTHFIELD, A., pp. 146–217. London: Academic Press.

SOKOLNIKOFF, I. S. & REDHEFFER, R. M. (1958). *Mathematics of Physics and Engineering*, pp. 257–260. New York: McGraw Hill.

VALDIOSERA, R., CLAUSSEN, C. & EISENBERG, R. S. (1974). Impedance of frog skeletal muscle fibres in various solution. *J. gen. Physiol.* **63**, 460–491.